NEOPLASIA
www.neoplasia.com

Volume 18 Number 11 November 2016 pp. 689–698 689

Tissue Transglutaminase Activates Cancer-Associated Fibroblasts and Contributes to Gemcitabine Resistance in Pancreatic Cancer[1,2,3]

Jiyoon Lee[*], Bakhtiyor Yakubov[†], Cristina Ivan[‡,§], David R. Jones[†], Andrea Caperell-Grant[†], Melissa Fishel[¶,#], Horacio Cardenas[**] and Daniela Matei[,††,‡‡]**

[*]Department of Otolaryngology–Head and Neck Surgery, Indiana University School of Medicine, Indianapolis, IN; [†]Department of Medicine, Indiana University School of Medicine, Indianapolis, IN; [‡]Department of Experimental Therapeutics, The University of Texas MD Anderson Cancer Center, Houston, TX; [§]Center for RNA Interference and Non-Coding RNAs, The University of Texas MD Anderson Cancer Center, Houston, TX; [¶]Department of Pediatrics, Indiana University School of Medicine, Indianapolis, IN; [#]Indiana University Melvin and Bren Simon Cancer Center, Indianapolis, IN; [**]Department of Obstetrics and Gynecology, Northwestern University Feinberg School of Medicine, Chicago, IL; [††]Robert H. Lurie Cancer Center, Chicago, IL; [‡‡]Jesse Brown VA Medical Center, Chicago, IL

Abstract

Resistance to chemotherapy is a hallmark of pancreatic ductal adenocarcinoma (PDA) and has been partly attributed to the dense desmoplastic stroma, which forms a protective niche for cancer cells. Tissue transglutaminase (TG2), a Ca^{2+}-dependent enzyme, is secreted by PDA cells and cross-links proteins in the tumor microenvironment (TME) through acyl-transfer between glutamine and lysine residues, promoting PDA growth. The objective of the current study was to determine whether secreted TG2 by PDA cells alters the response of pancreatic tumors to gemcitabine. Orthotopic pancreatic xenografts and co-culture of PDA and stromal cells were employed to determine the mechanisms by which TG2 alters tumor-stroma interactions and response to gemcitabine. Analysis of the pancreatic The Cancer Genome Atlas (TCGA) database demonstrated that increased TG2 expression levels correlate with worse overall survival (hazard ratio = 1.37). Stable TG2 knockdown in PDA cells led to decreased size of pancreatic xenografts and increased sensitivity to gemcitabine *in vivo*. However, TG2 downregulation did not increase cytotoxicity of gemcitabine *in vitro*. Additionally, multivessel density and gemcitabine uptake in pancreatic tumor tissue, as measured by mass spectrometry (MS-HPLC), were not significantly different in tumors expressing TG2 versus tumors in which TG2 was knocked down. Fibroblasts, stimulated by TG2 secreted by PDA cells, secrete laminin A1, which protects cancer cells from gemcitabine-induced cytotoxicity. In all, our results demonstrate that TG2 secreted in the pancreatic TME orchestrates the cross talk between cancer cells and stroma, impacting tumor growth and response to chemotherapy. Our study supports TG2 inhibition to increase the antitumor effects of gemcitabine in PDA.

Neoplasia (2016) 18, 689–698

Address all correspondence to: Daniela Matei, MD, Professor, Department of Obstetrics and Gynecology, Northwestern University Feinberg School of Medicine, 303 E Superior Street, Lurie 4-107, Chicago, IL, 60611.
E-mail: daniela.matei@northwestern.edu

[1] Grant support: This work was made possible by funding from the National Cancer Institute (award CA152502 to D.M.), the US Department of Veterans Affairs (to D.M.), a Project Development Team within the ICTSI NIH/NCRR (grant number UL1TR001108), and the IUPUI Signature Center Initiative. The analytical work was performed in the Clinical Pharmacology Analytical Core, a shared facility of the Indiana University Melvin and Bren Simon Cancer Center supported by the National Cancer Institute grant P30 CA082709.
[2] Financial support: National Cancer Institute (award CA152502) to D. M.
[3] Conflicts of interest: The authors disclose no potential conflicts of interest.
Received 25 May 2016; Revised 12 September 2016; Accepted 15 September 2016

1476-5586
http://dx.doi.org/10.1016/j.neo.2016.09.003

Introduction

Pancreatic ductal adenocarcinoma (PDA) is the fourth leading cause of cancer mortality in the world [1]. PDA metastasizes early and is resistant to currently available therapy [2,3]. A hallmark of pancreatic cancer is the dense desmoplastic stroma composed of activated myofibroblasts, pancreatic stellate cells, collagen, and other extracellular matrix (ECM) proteins [4–6]. Tissue transglutaminase (TG2), a calcium (Ca^{2+})-dependent enzyme that catalyzes protein transamidation through acyl-transfer between glutamine and lysine residues, is abundantly expressed in pancreatic cancer cells and secreted in the pancreatic stroma. We recently showed that TG2 contributes to pancreatic cancer progression by modulating the tumor microenvironment (TME) through collagen cross-linking, which in turn stimulates proliferation and activation of fibroblasts [7]. This fibroblast and TG2-mediated cross-linked collagen- rich stroma in turn stimulates tumor growth by activating the Yes-associated protein and transcriptional co-activator with PDZ-binding motif oncogenic signaling. Here, we set out to determine whether stroma modifications induced by TG2 also alter the response of pancreatic tumors to chemotherapy.

Previous reports have shown that TG2 overexpression in pancreatic tumors is associated with poor clinical outcomes and resistance to chemotherapy [3,8]. Resistance to anticancer agents is generally attributed to intra- or extracellular cellular mechanisms. Intracellular mechanisms of resistance in PDA include overexpression of the P-glycoprotein and of other transporters [9,10] or activation of antiapoptotic proteins, such as Bcl-xL and NF-κB [11,12]. Previous studies attributed TG2-induced resistance to gemcitabine to activation of the NF-κB survival signaling and of the focal adhesion kinase/phosphatidylinositol 3-kinase/AKT signaling pathways [3,8]. Extracellular mechanisms of resistance involve interactions between tumor cells and the surrounding stroma, which provide cancer cells with powerful survival cues protecting them from chemotherapy- or radiation-induced apoptosis [13,14]. Recent reports have suggested that inefficient drug delivery within the pancreatic milieu due to the dense stroma contributes to resistance to chemotherapy [15]. Here, we examined how the interplay between cancer and stromal cells mediated by TG2 secreted within the TME contributes to resistance to gemcitabine.

TG2 is a multifunctional protein, whose roles are regulated by subcellular localization and environmental factors, Ca^{2+} and GTP being the two key regulators [16–18]. TG2 binding of Ca^{2+}, typically in the ECM, causes an extended (open) conformation exposing the catalytic core, which promotes the enzymatic activity and inhibits the binding and hydrolysis of GTP. On the contrary, TG2 binding of GTP in the intracellular space induces a compact (closed) conformation and inhibits the catalytic activity [19]. In the cytoplasm where Ca^{2+} concentration is low, the transamidating activity is inhibited [18,20], whereas in the extracellular compartment, where Ca^{2+} concentration is high, TG2 is enzymatically active and modifies extracellular proteins by cross-linking [21]. Here, we focused on the functions of TG2 in the ECM of pancreatic tumors.

By using co-culture system and pancreatic orthotopic xenografts, we demonstrate that TG2 knockdown in PDA cells inhibited response to gemcitabine *in vivo* but not *in vitro*. This discrepancy suggests that its effects occurred primarily through modulation of the TME. The co-culture of PDA cells with fibroblasts stimulated cancer cell proliferation, and TG2-mediated cross-linked collagen stimulated the proliferation of cancer-associated myofibroblasts. Cancer-associated fibroblasts co-cultured with cancer cells in which TG2 was knocked down secrete decreased levels of laminin 1, which in turn partly protected PDA cells from gemcitabine-induced cytotoxicity. Collectively, our data support that TG2 facilitates the cross talk between cancer and stromal cells, thereby modulating response to chemotherapy.

Materials and Methods

Chemicals and Reagents

Antibodies for TG2 (NeoMarkers, Fremont, CA; #CUB7402) and GAPDH (Meridian Life Science, Inc., Memphis, TN) were used for Western blotting at dilutions of 1:1000 and 1:20,000, respectively. Antibodies for TG2 (NeoMarkers; #RB-060-P1ABX), Laminin 1, Ki67, and CD31 (Abcam, Cambridge, MA) were used for immunohistochemistry (IHC) at a dilution of 1:50 and or 1:100.

Cell Culture

AsPC1 and BxPC3 cells were purchased from the American Type Culture Collection (Rockville, MD), Panc1 and MIA PaCa-2 (Paca2) cells were a gift from Prof. Murray Korc (Indiana University Melvin and Bren Simon Cancer Center [IUSCC], Indianapolis, IN), and green fluorescence protein (GFP) expressing AsPC1 (GFP-AsPC1) cells were provided by Dr. Jingwu Xie (IUSCC, Indianapolis, IN). Human pancreatic stellate cells (hPSCs) were obtained from ScienCell Research Laboratories (Carlsbad, CA), GFP-expressing human neonatal dermal fibroblasts (GFP-HNDFs) were purchased from Angioproteome (Boston, MA), and normal human dermal fibroblasts (NHF544) were provided by Dr. Dan Spandau (IUSCC, Indianapolis, IN). Human pancreatic cancer-associated fibroblasts (CAFs; UH1303-35) were isolated from a human pancreatic tumor by using the outgrowth method and immortalized by transduction of telomerase (hTERT). AsPC1, GFP-AsPC1, and BxPC3 cells were cultured in RPMI 1640 medium (Cellgro, Manassas, VA) supplemented with 10% fetal bovine serum and 1% antibiotics. Panc1, Paca2, hPSCs, GFP-HNDFs, NHF544, and CAFs were grown in Dulbecco's modified Eagle's medium (Cellgro) supplemented with 10% fetal bovine serum and 1% antibiotics. Cells were grown at 37°C under 5% CO_2. Conditioned medium was collected after 24-hour incubation of 5×10^5 PDA cells in 1 ml of serum-free RPMI medium. Debris was removed by centrifugation at 1200 rpm for 5 minutes. Laminin (Sigma-Aldrich, St. Louis, MO) diluted with sterile Hank's balanced salt solution (HBSS) was used to coat 96-well plates at 5 to 10 μg/cm^2 for 2 hours at 37°C. PDA cells were plated on this matrix at a density of 2.5×10^3 to 2×10^4 cells per well for 16 hours (O/N). Gemcitabine (Eli Lilly, Indianapolis, IN) treatment was applied at the indicated concentrations.

Co-Culture

For indirect co-culture, 3.5×10^5 hPSCs were cultured in the CM collected from PDA cells for 48 hours. RNA isolated from the hPSCs was used for gene expression analysis employing the RT^2 Profiler PCR Array. For direct co-culture, 5×10^3 GFP-AsPC1 cells and 5×10^3 NHF544 were mixed and co-cultured in a 96-well plate for 96 hours. In addition, 1.5×10^4 GFP-AsPC1 cells and 1.5×10^4 CAFs were mixed and co-cultured in 24-well plates for 48 hours.

Proliferation Assays

Cell counting kit (CCK)-8 (Dojindo Molecular Technologies, Inc., Rockville, MD) was used to determine the proliferation of PDA cells and CAFs according to the manufacturer's instructions.

Absorbance at 450 nm was measured using an EL800 microplate reader (BioTek Instruments, Inc., Winooski, VT). The CCK-8 cell counting kit or the bromodeoxyuridine cell proliferation enzyme-linked immunosorbent assay kit (Abcam) was used to measure proliferation of PDA cells cultured on laminin. Absorbance at 370 nm (reference wavelength, 492 nm) was measured by SPECTRAmax Plus 384 microplate spectrophotometer (Molecular Devices, Sunnyvale, CA). Proliferation of GFP-AsPC1 cells in a direct co-culture with NHF544 was measured every 24 hours for 96 hours by assessing fluorescence intensity (relative fluorescence units) using the SpectraMax Gemini XS microplate fluorometer (Molecular Devices) at 485-nm excitation and 538-nm emission. LUNA-FL Automated Fluorescence Cell Counter (Logos Biosystems, Inc., Annandale, VA) was used to assess the alive GFP-AsPC1 cells in a direct co-culture with CAFs after 48 hours of gemcitabine treatment by counting the number of GFP-expressing cells. The assays were repeated three times.

Cell Transfection

TG2 was stably knocked down in AsPC1 and BxPC3 cells by transducing MISSION shRNA Lentiviral Transduction Particles (Sigma-Aldrich) as previously described [7]. Briefly, the PDA cells were transduced with scrambled shRNA (shCtrl) or shTG2, followed by polyclonal selection with puromycin (1 μg/ml). TG2 knockdown was confirmed by Western blotting.

Western Blotting

Cells were lysed in radioimmunoprecipitation assay buffer containing Halt protease inhibitor cocktail (Thermo Scientific, Waltham, MA). Equal amounts of proteins were separated by sodium dodecyl sulfate polyacrylamide gel electrophoresis and transferred to polyvinylidene difluoride membranes (Bio-Rad Laboratories, Inc., Hercules, CA). After blocking, membranes were blotted with primary antibodies followed by HRP-conjugated secondary antibodies. The protein-antibody complexes were visualized by enhanced chemiluminescence solution (Thermo Fisher Scientific), and images were captured by ImageQuant LAS 4000 mini imager with a Chemilux CCD camera (GE Healthcare, Uppsala, Sweden). The shRNA effects were quantified by densitometry by using ImageJ software. All analyses were repeated at least three times.

Orthotopic Pancreatic Xenograft Mouse Model

Animal experiments were conducted after review and approval by the IU Animal Care and Use Committee and were in compliance with federal regulations. Briefly, 1.5×10^5 AsPC1 cells, stably transduced with shRNA targeting TG2 or scrambled shRNA (shCtrl; control), diluted in 50 μl of medium were injected into the tail of pancreas of 7- to 8-week-old female nude mice (nu/nu Balbc) from Harlan (Indianapolis, IN) using a 27.5-gauge needle under isoflurane anesthesia, as previously described [7]. Gemcitabine at a concentration of 25 mg/kg or PBS (control) was administered to tumor-bearing mice (n = 7 per PBS group and n = 8 per gemcitabine group) twice a week for 4 weeks *via* intraperitoneal injection. Mice were euthanized after 4 weeks, and tumor weights, volumes, and numbers of metastases were assessed. Tumors were measured three-dimensionally, and tumor volumes were calculated as $4/3*\pi*(L/2)*(W/2)*(H/2)$, where L is length, W is width, and H is height. Metastatic implants were counted. To determine gemcitabine distribution in tissue, gemcitabine was administered as a single dose (25 mg/kg) *via* intravenous (iv) injection to tumor-bearing mice 4 weeks after PDA cell implantation (shCtrl; n = 5, shTG2; n = 6). Mice were euthanized 2 minutes after gemcitabine administration [22], and tumors and plasma were immediately collected and processed.

Gemcitabine Concentration Measurement

Tumors were harvested and homogenized in phosphate buffer containing tetrahydrouridine, a cytidine deaminase inhibitor, to prevent the degradation of gemcitabine to 2′,2′-difluorodeoxyuridine (dFdU). Liquid-liquid extraction, internal standardization (5-azacytidine), and HPLC–tandem mass spectrometry was used to measure gemcitabine and dFdU in tumor tissue and plasma. Tumor homogenates in tetrahydrouridine-containing phosphate buffer were extracted with ethyl acetate, the extract was transferred to a different tube, and the ethyl acetate was evaporated to dryness. Mobile phase was added to each tube, an aliquot was injected into the HPLC, and the compounds were separated using a C8 column (5 μm; 4.6 × 250 mm Zorbax). Compounds were detected by electrospray ionization tandem mass spectrometry in positive mode (Thermo Quantum Ultra; Thermo Fisher) using 264/112, 265/113, and 245/113 as the Q1/Q3 for gemcitabine, dFdU, and 5-azacytidine, respectively. The lower limit of quantification was 1 ng/ml and 30 ng/ml for gemcitabine and dFdU, respectively.

Immunohistochemistry

Paraffin-embedded orthotopic pancreatic xenografts were deparaffinized and immunostained with TG2 polyclonal (Neomarkers), Laminin 1, Ki67, or CD31 (Abcam) antibodies after sodium citrate antigen retrieval. Secondary labeling was based on the Avidin/Biotin system (Dako North America, Inc.). Slides were stained with 3,3′-diaminobenzidine and counterstained with hematoxylin. Negative controls were run in parallel, with isotype IgG control. Microvessel density (MVD) was counted at the interface with stroma or, if no adjacent normal tissue was present, at the edge of the tissue section. Multiple (8 to 18) 200× fields were counted on an Olympus BX51 microscope around the entire perimeter of the largest section of tumor present on the slide. CD31 immunoreactivity alone was not considered sufficient for identification of a vessel, as nonspecific staining was observed in zones of necrosis, in plasma cells, and occasionally within the tumor cells. A vessel was counted when a CD31-positive structure formed a lumen, had associated cells morphologically consistent with endothelial cells, or contained erythrocytes. Percentages of Ki67-staining cells relative to all nuclei were counted in five 100× fields per specimen, and average counts were calculated. Slides were reviewed and scored by a board-certified pathologist.

RT² Profiler PCR Array

The human Extracellular Matrix and Adhesion Molecules RT^2 Profiler PCR Array was purchased from SA Bioscience (Valencia, CA), and quantitative reverse transcriptase polymerase chain reaction (qRT-PCR) was performed on ABI Prism 7900 HT (Applied Biosystems, Foster City, CA) according to the manufacturer's instructions.

Quantitative Real-Time PCR

Total RNA was isolated using RNA STAT-60 Reagent (Tel-Test Inc., Friendswood, TX) and reverse-transcribed using iScript cDNA synthesis kit (Bio-Rad Laboratories, Inc.). The primers for qRT-PCR were: *LAMA1* forward: AGG AGT GGG TGT GTG ACG A and reverse: CCA GGC AGT TGG CTC TAA TC and *GAPDH* forward: AGC CAC ATC GCT CAG ACA C and reverse: GCC

CAA TAC GAC CAA ATC C. Relative target gene expression was calculated using Ct method, $2^{-\Delta Ct} = 2^{-[Ct(CTGF) - Ct(GAPDH)]}$, where Ct is the *cycle threshold value* defined as the fractional cycle number at which the target fluorescent signal passes a fixed threshold. All experiments were performed in duplicates in three independent experiments, and results are presented as means ± standard error (SE) of replicates.

Statistical Analysis

Student's *t* test was used to compare measurements between groups. *P* values < .05 were considered significant. For the survival analysis, *mRNA* expression level data (Level 3 Illumina RNASeqv2), publicly available from TCGA (http://tcgadata.nci.nih.gov/) for 178 patients with pancreatic adenocarcinoma, were used. The clinical information was retrieved from cbioPortal (http://www.cbioportal.org/). The overall survival information was complete for 76 patients. Statistical analyses were performed in R (version 3.0.1) (http://www.r-project.org/), and the statistical significance was defined as a *P* value less than .05. We performed Cox regression analysis as an initial screen for associations between survival and *TG2 mRNA* expression. We observed an association between *TG2* expression and shorter overall survival: hazard ratio (HR) = 1.37, 95% confidence interval (CI) = 1.02-1.85, and *P* value (Wald test) = .0377. We then used the log-rank test to find the point (cutoff) with the most significant (lowest *P* value) split in high- and low-*TG2* groups. The Kaplan-Meier plots were generated for this cutoff (0.75) (*P* = .025). The numbers of patients at risk in low-/high-*TG2* groups at different time points are presented at the bottom of the graph. The Spearman's rank-order correlation test was applied to measure the strength of the association between *TGM2* and *LAMA1*.

Results

TG2 Expression and Response to Gemcitabine In Vitro

Endogenous TG2 expression levels were measured in PDA cell lines and in fibroblasts (GFP-HNDF) by immunoblotting (Figure 1*A, upper*). Among PDA cells, AsPC1 and BxPC3 cells expressed relatively abundant TG2, whereas Panc1 and Paca2 cells expressed relatively low TG2 levels. Fibroblasts also expressed endogenous TG2, consistent with our previous observations demonstrating TG2 expression in PDA-associated stroma [7]. TG2 was knocked down in AsPC1 and BxPC3 cells by stably transducing shRNA targeting TG2 (shTG2). TG2 expression levels were significantly decreased in cells stably transduced with shTG2 compared with cells transduced with scrambled shRNA (shCtrl; Figure 1*A, lower*).

To determine whether TG2 expression is associated with clinical outcomes in patients with PDA, the publically available database associated with the pancreatic cancer TCGA project was analyzed. Tumors with high TG2 expression levels were associated with poor survival compared with those expressing low TG2 (Figure 1*B*, HR = 1.37, 95% CI = 1.02-1.85, *P* = .0377). These data suggest that TG2 expression alters clinical outcome either by impacting tumor progression or by altering response to treatment.

To measure the effects of TG2 on cell proliferation and response to gemcitabine, cell proliferation was assessed in PDA cells in which TG2 expression was knocked down by using shRNA. Interestingly, TG2 knockdown did not alter proliferation of AsPC1 (Figure 1*C*) or BxPC3 cells (Figure 1*D*). Likewise, TG2 knockdown did not significantly alter the response of AsPC1 (Figure 1*E*) or BxPC3 cells (Figure 1*F*) to gemcitabine, suggesting that the enzyme does not have a measurable impact on cell growth and sensitivity to gemcitabine *in vitro*.

TG2 Expression and Response to Gemcitabine In Vivo

We next tested whether knockdown of TG2 in PDA cells induces sensitivity to gemcitabine *in vivo*. For this, we used orthotopic pancreatic xenografts derived from AsPC1 + shCtrl or + shTG2 cells. After cell implantation, mice were treated with gemcitabine twice a week for 4 weeks at a dose of 25 mg/kg *via* intraperitoneal injection ($n = 7$ per PBS group and $n = 8$ per gemcitabine group). In concordance with our previous data [7], average tumor volumes and weights were significantly decreased in xenografts derived from AsPC1 + shTG2 cells compared with controls (Figure 2*A*, *left* and *middle*, *P* = .002 and *P* = .001, respectively), whereas there was no significant difference in the number of macrometastases between the two groups (Figure 2*A*, *right*, *P* = .55). Gemcitabine treatment decreased the average tumor volume and weight in both AsPC1 + shCtrl–and AsPC1 + shTG2–derived xenografts compared with PBS (Figure 2*A*, *left* and *middle, P* < .002). Furthermore, average tumor volume and weight were lower in AsPC1 + shTG2–derived xenografts treated with gemcitabine compared with controls treated with gemcitabine (Figure 2*A*, *left* and *middle*, *P* = .01 and *P* = .03, respectively). In addition, gemcitabine treatment significantly decreased number of macrometastases in mice bearing AsPC1 + shTG2 xenografts compared with mice carrying AsPC1 + shCtrl tumors (Figure 2*A*, *right, P* = .005). Together, these data suggest that TG2 knockdown *in vivo* inhibits tumor growth and that the combination of TG2 knockdown and gemcitabine induces the most significant reduction in tumor burden.

Stable knockdown of TG2 in pancreatic xenografts was confirmed by IHC, and the effect of TG2 knockdown on cell proliferation *in vivo* was determined by immunostaining for Ki67 in xenografts (Figure 2*B*, *upper*). In contrast to the *in vitro* results showing no effects of TG2 knockdown on PDA cell proliferation, the number of Ki67-positive PDA cells in AsPC1 + shTG2 xenografts was significantly decreased compared with that of control tumors (Figure 2*B*, *lower*, $n = 3$ per group, *P* = .042). Additionally, tumor vascularization was assessed by counting the number of vascular structures detectable through CD31 immunostaining in AsPC1 + shTG2 and control xenografts. No significant MVD difference was detectable between groups (Figure 2*C*, $n = 6$ per group, *P* = .2).

TG2 Expression and Penetrance of Gemcitabine in Tumor Tissues

Based on our previous findings showing decreased fibrosis in pancreatic tumors derived from PDA cells in which TG2 was stably knocked down [7], we sought to determine whether the more pronounced gemcitabine effects were due to increased penetrance of gemcitabine. To determine gemcitabine concentrations in tumor tissue depending on TG2 expression levels, we used orthotopic pancreatic xenografts derived from AsPC1 + shCtrl and + shTG2 cells. Four weeks after PDA cell implantation, when tumors were formed, mice were given a single iv gemcitabine dose of 25 mg/kg prior to tumor harvest within 2 minutes. The uptake of gemcitabine in the pancreas occurs within minutes after iv administration, and gemcitabine gets rapidly excreted [22,23]. The sum of gemcitabine and dFdU concentrations in tumor tissues was slightly higher in the AsPC1 + shTG2 xenografts compared with controls but did not reach statistical significance (Figure 2*D*, shCtrl; $n = 5$ and shTG2; $n = 6$, *P* = .4). Plasma gemcitabine and dFdU

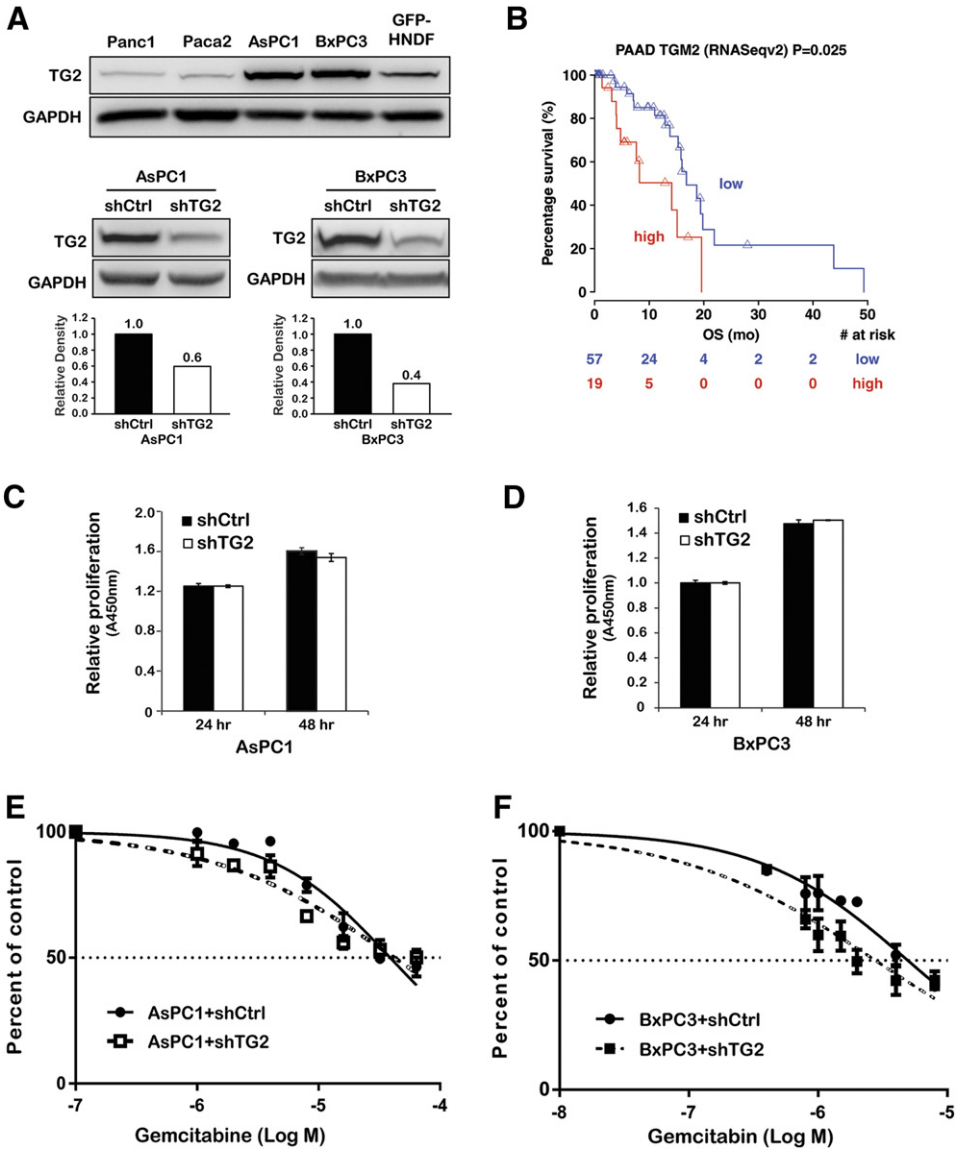

Figure 1. TG2 expression and response to gemcitabine *in vitro*. (A) Western blotting for TG2 and GAPDH (internal control) in PDA cells, fibroblasts (upper), and PDA cells stably transduced with shRNA targeting TG2 (shTG2) or scrambled shRNA (shCtrl; lower). The bar graphs represent quantification of TG2 knockdown in AsPC1 and BxPC3 cells by densitometry. (B) Kaplan-Meier survival plots of patients with PDA according to the TG2 expression level. The numbers of patients at risk in low-/high-TG2 groups at different time points are presented at the bottom of the graph.Relative proliferation of AsPC1 + shCtrl and + shTG2 cells (C) and BxPC3 + shCtrl and +shTG2 cells (D) at 24 and 48 hours of culture (CCK-8 assay).Dose-response curves representing percentage of surviving AsPC1 + shCtrl and + shTG2 cells (E) and BxPC3 + shCtrl and + shTG2 cells (F) after 48 hours of gemcitabine treatment (CCK-8 assay).

concentrations were similar between the groups (data not shown). This nonsignificant trend could reflect the variability observed within groups and does not completely exclude an effect of TG2 knockdown on gemcitabine tissue penetrance. Taken altogether, our findings demonstrate that the effects of TG2 on tumor growth and response to gemcitabine are not due to the direct effects of TG2 on PDA cells or to altered tumor vascularity and intratumoral drug delivery.

Effects of Gemcitabine in Co-Culture of PDA Cells with Fibroblasts

To determine whether the effects of TG2 on tumor growth and response to gemcitabine *in vivo* could be mediated by the stromal fibroblasts, we assessed their effects on PDA cell proliferation and response to chemotherapy. Co-culture of GFP-AsPC1 cells with NHF544 fibroblasts (ratio of 1:1) showed increased proliferation of PDA cells grown in the presence of fibroblasts compared with AsPC1 cells cultured alone (Figure 3*A*, $P < .05$). As we have previously shown that TG2-expressing tumors are enriched in cross-linked collagen 1 [7], we next sought to determine whether the presence of collagen stimulates fibroblast proliferation. For this, we used immortalized pancreatic CAFs cultured on uncoated plates or on plates coated with either native collagen 1 or TG2-mediated cross-linked collagen 1. The proliferation of CAFs was increased on collagen-coated compared with uncoated plates (Figure 3*B*, $P = .01$) and even more on TG2-mediated cross-linked collagen compared with native collagen (Figure 3*C*, $P < .001$). Next, a co-culture experiment determined the effects of fibroblasts on PDA cell response to increasing doses of gemcitabine. The number of surviving

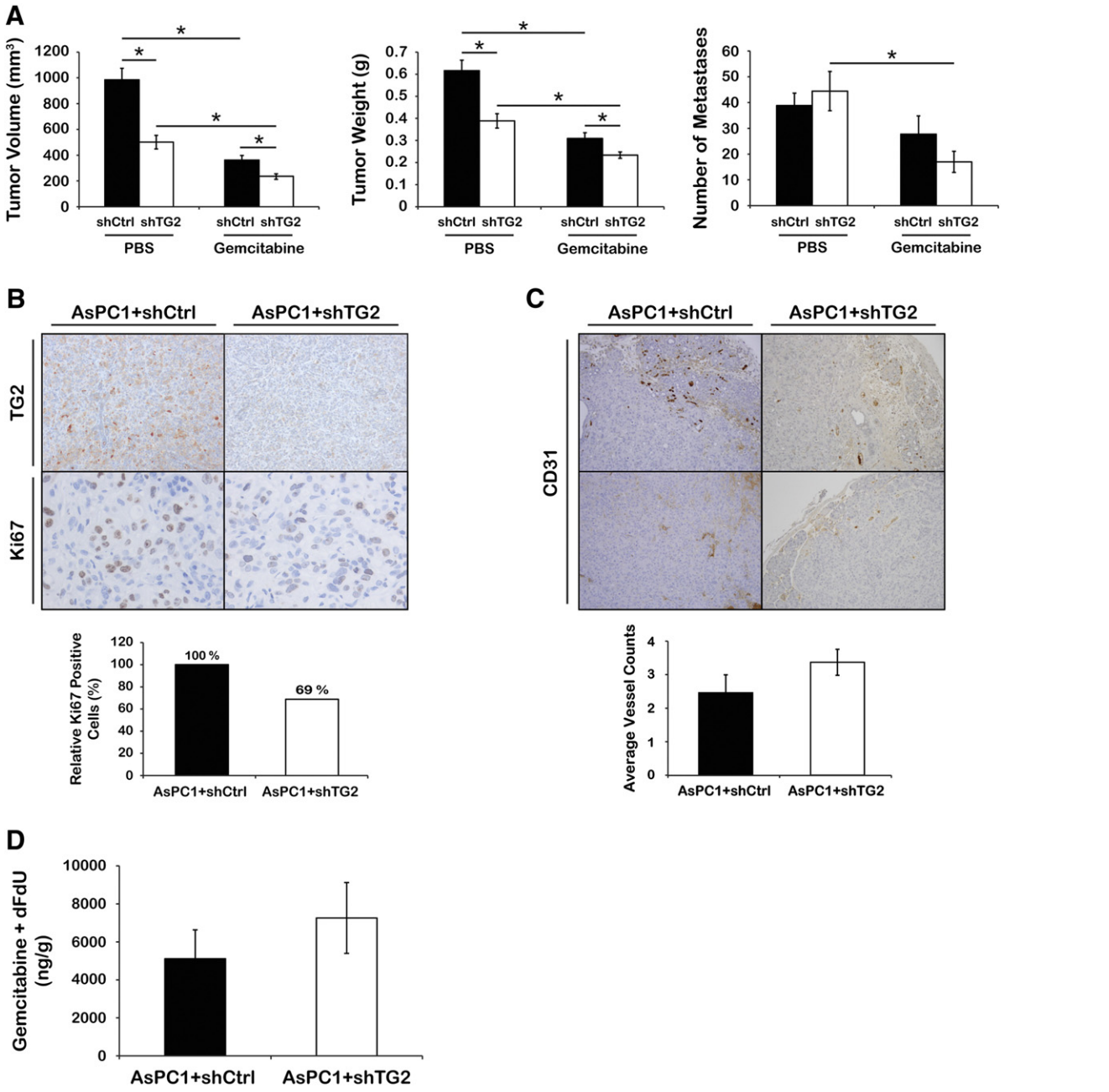

Figure 2. TG2 expression and response to gemcitabine *in vivo.* (A) Average tumor volumes (left), weights (middle), and numbers of metastases (right) of xenografts derived from AsPC1 + shCtrl and + shTG2 cells and treated with gemcitabine ($n = 8$) or PBS ($n = 7$). Bars represent average measurements ± SE. *$P < .05$. (B) IHC for TG2 and Ki67 (upper) and a graph representing relative percentage of Ki67-positive cells (lower, $n = 3$ per group, $P = .042$) in AsPC1 + shCtrl and + shTG2 xenografts. Ki67-positive cells were counted in five fields per sample. (C) IHC for CD31 (upper) and a graph representing average number of vessels counted (lower) in AsPC1 + shCtrl and + shTG2 xenografts ($n = 6$ per group, $P = .2$). Bars represent average vessel counts ± SE. (D) Sum of gemcitabine and dFdU concentration per tumor weight (ng/g) in AsPC1 + shCtrl and + shTG2 xenografts (shCtrl; $n = 5$ and shTG2; $n = 6$, $P = .4$). Bars represent average concentrations ± SE.

GFP-AsPC1 cells cultured alone was significantly decreased after gemcitabine treatment compared with those cultured in the presence of fibroblasts (Figure 3*D*, $P < .05$), supporting a protective effect of stromal cells against gemcitabine.

Effects of Laminin A1 Secreted by Stromal Cells on Gemcitabine-Induced Cytotoxicity

To determine the mechanism by which TG2 secreted by PDA cells modifies fibroblasts to induce a protective tumor environment, a qRT-PCR array was used to compare *mRNA* expression levels of stroma-associated genes in hPSCs cultured with CM from AsPC1 cells stably transduced with shRNA targeting TG2 or controls (Figure 4*A*). Of 84 genes measurable in the array, 4 transcripts were downregulated more than twofold in hPSCs indirectly co-cultured with AsPC1 + shTG2 cells compared with control AsPC1 cells. These transcripts include *laminin A1 (LAMA1), collagen 12A1, MMP12,* and *NCAM1* (Figure 4*B*). Decreased *mRNA* expression of *LAMA1* was confirmed by qRT-PCR in hPSCs co-cultured with CM from AsPC1 + shTG2 cells compared with that from AsPC1 + shCtrl cells (Figure 4*C*, $P < .05$) and in AsPC1 + shTG2

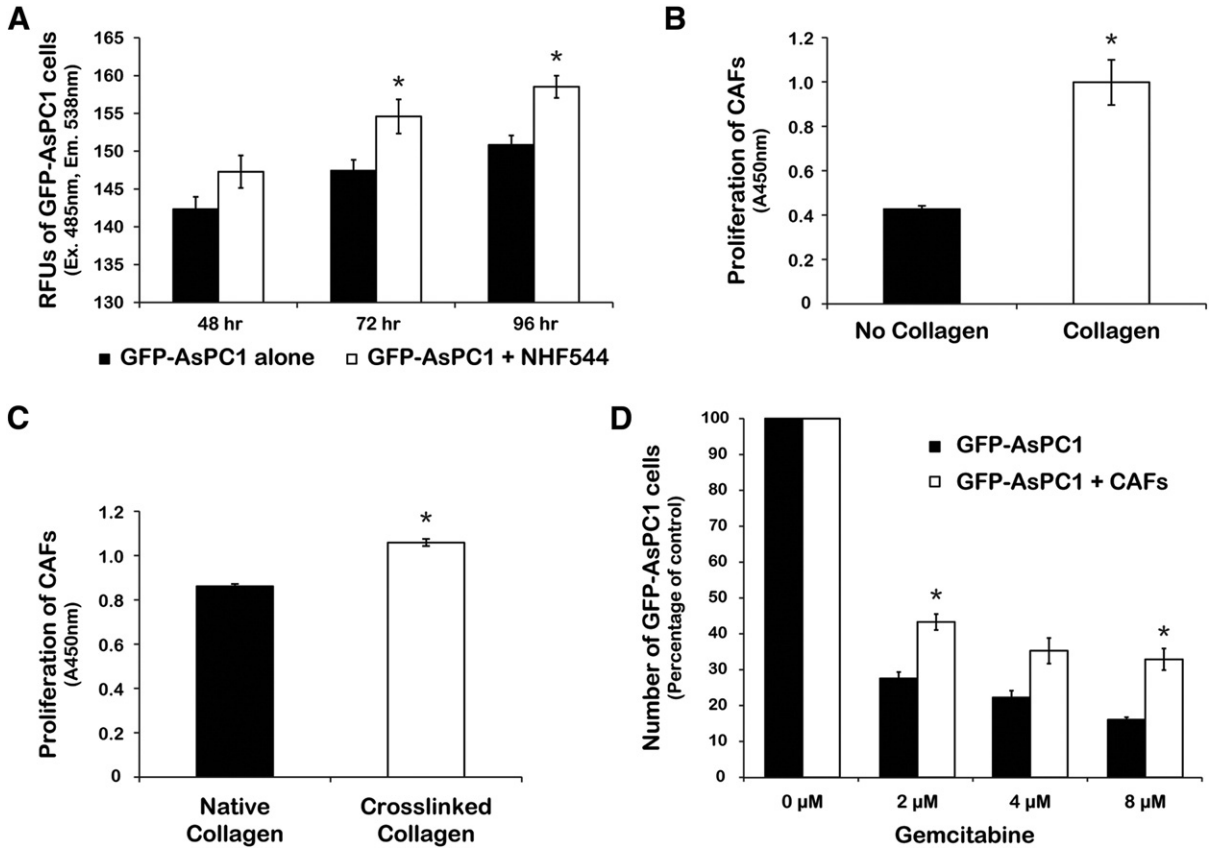

Figure 3. Fibroblasts modulate the response of PDA cells to gemcitabine *in vitro*. (A) Proliferation of GFP-AsPC1 cells in co-culture with NHF544 or cultured alone. Green fluorescence in GFP-AsPC1 cells was measured at 485-nm excitation and 538-nm emission. Bars represent average relative fluorescence units of triplicates ± SE. *$P < .05$. Proliferation of CAFs (CCK-8 assay) cultured for 48 hours on collagen-coated or uncoated plates (B, $P = .01$) and on native or TG2-mediated cross-linked collagen (C, $P < .001$). Bars represent average measurements ± SE. (D) Relative number of alive GFP-AsPC1 cells cultured alone or with CAFs after 48 hours of gemcitabine treatment. Bars represent average measurements ± SE. *$P < .05$.

pancreatic xenografts compared with controls (Figure 4*D*, $n = 4$ per group, $P < .05$). Furthermore, decreased LAMA1 protein expression level, as measured by IHC, was observed in AsPC1 + shTG2 pancreatic xenografts compared with control xenografts (Figure 4*E*), confirming the association. To test whether a direct correlation between *LAMA1* and *TG2* gene expression also exists in human pancreatic tumors, the publically available TCGA database was explored. A significant correlation between *TG2* and *LAMA1* expression levels was demonstrated by the Spearman's rank-order correlation test (Figure 4*F*, $P = .002$), suggesting relevance in human tumors.

To examine the functional effects of laminin on the growth of PDA cells, AsPC1, BxPC3, or Panc1 cells were cultured on plates coated with 5 μg/cm^2 of laminin or on uncoated plates. After 48 hours of culture, no significant difference was observed among AsPC1, BxPC3, and Panc1 cells grown on laminin-coated versus uncoated plates (Figure 4*G*). We next examined the effects of laminin on proliferation of cells treated with gemcitabine. A partial protective effect against gemcitabine-induced cytotoxicity was observed when BxPC3 cells were grown on laminin-coated plates compared with uncoated plates (Figure 4*H*). In contrast, collagen 1 or TG2-mediated cross-linked collagen did not alter the response of PDA cells to gemcitabine (Supplementary Figure 1). Collectively, our data support that TG2 secreted by PDA cells promote fibroblast proliferation and secretion of specific stromal factors, such as LAMA1, which in turn contribute to the protection of cancer cells from the cytotoxic effects of chemotherapy (Figure 5).

Discussion

Together with our previous results [7], these data support that TG2 regulates the interaction between PDA and stromal cells in pancreatic cancer, altering tumor progression and response to gemcitabine. Here, we show that the combination of TG2 knockdown and gemcitabine decreased tumor volumes and number of metastases in PDA xenografts. Given that the effects of TG2 knockdown on responsiveness to gemcitabine were not detectable *in vitro*, we speculated that the *in vivo* effects were mediated through PDA-associated desmoplasia.

Indeed, we have previously shown that TG2 secreted by PDA cells activates fibroblasts and stimulates their proliferation [7]. We demonstrated that one of the mechanisms through which TG2 promoted the growth of fibroblasts occurred by collagen cross-linking in the stroma [7]. Other groups have also shown that activation and proliferation of stellate cells in the pancreatic milieu contribute to the growth and invasiveness of pancreatic tumors [24,25]. Here we demonstrate that TG2 knockdown in PDA cells also causes decreased laminin secretion from fibroblasts, which contribute to increased sensitivity to gemcitabine. Laminin is a key component of the

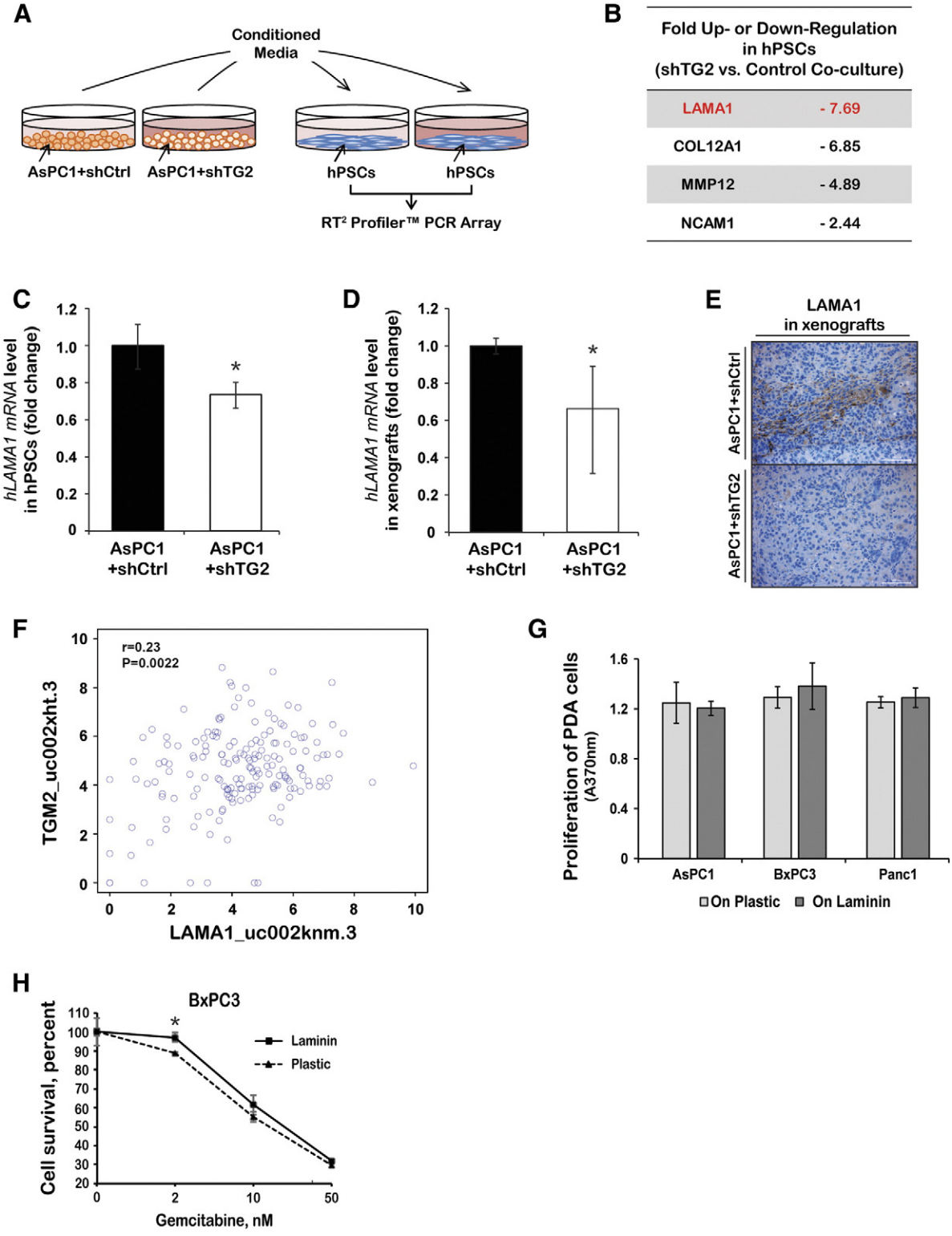

Figure 4. Cross-talk between PDA and stromal cells mediated by TG2. (A) Schematic of the indirect co-culture experiment. hPSCs were cultured with CM collected from AsPC1 + shCtrl and + shTG2 cells. RNA isolated from hPSCs was used for cDNA synthesis followed by gene expression analysis using the RT^2 Profiler PCR Array. (B) List of genes differentially expressed in hPSCs cultured with AsPC1 + shTG2 CM compared with + shCtrl CM.qRT-PCR measured *LAMA1 mRNA* levels in hPSCs cultured with CM from AsPC1 + shCtrl or + shTG2 cells (C) and in xenografts derived from AsPC1 + shCtrl or + shTG2 cells (D, $n = 4$ per group). Bars represent average fold changes ± standard deviation. *$P < .05$. (E) Representative IHC images of LAMA1 (laminin 1) in AsPC1 + shCtrl and + shTG2 xenografts. (F) Spearman's rank-order correlation measured the correlation between *TG2* and *LAMA1 mRNA* expression levels in human PDA specimens from the TCGA database ($P = .002$). (G) Proliferation of AsPC1, BxPC3, and Panc1 cells cultured for 48 hours on laminin-coated or uncoated plates (bromodeoxyuridine assay). Bars represent average measurements ± SE. (H) Relative proliferation of BxPC3 cells cultured on laminin-coated or uncoated plates and treated with gemcitabine for 96 hours (CCK8 assay). Bars represent average measurements ± SE. *$P < .05$.

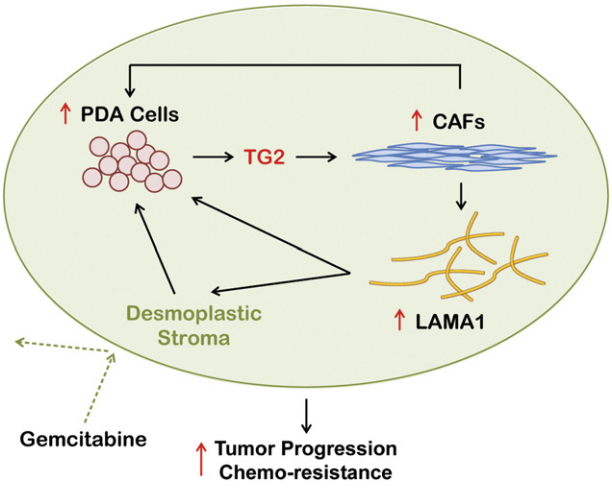

Figure 5. Model illustrating the proposed interactions between tumor and stroma cells mediated by TG2 in PDA.

pancreatic ECM, and PDA cell adhesion to laminin [26,27] with subsequent activation of signaling pathways, particularly through activation of focal adhesion kinase, has been implicated in resistance to chemotherapy [3,26].

Our findings are consistent with a previous report by Verma et al. demonstrating that siRNA-mediated knockdown of TG2 inhibited pancreatic tumor growth and enhanced gemcitabine therapeutic efficacy [28]. By delivering gemcitabine alone or in combination with TG2-specific siRNA-DOPC (1,2-dioleoyl-sn-glycero-3-phosphatidylcholine) liposomes to pancreatic tumors–bearing mice, Verma et al. demonstrated that knockdown of TG2 significantly sensitized tumors to chemotherapy, decreased tumor growth, and inhibited metastasis. In addition, TG2 inhibition by liposomes carrying siRNA targeting TG2 reduced cell proliferation, angiogenesis, and phosphorylation of AKT. Our findings differ from the previous report, as we did not observe inhibition of metastasis or changes in tumor MVD induced by TG2 knockdown. These differences may be related to the different approaches to TG2 downregulation in the two studies, as the liposomal delivery of siRNA in the peritoneal cavity could have contributed to nonspecific targeting of TG2 expression in nontumor tissue, such as the stroma and endothelial cells. These effects of the TG2-targeting siRNA-DOPC could account for the antiangiogenic effects observed and the subsequent inhibition of cell proliferation, tumor growth, and metastasis. Consistent with the lack of effect on tumor vasculature, we observed that the uptake of gemcitabine in pancreatic tissue after iv administration was not significantly different in AsPC1 + shTG2 xenografts compared with controls. Although a trend toward increased gemcitabine concentrations in tumor tissue derived from PDA cells in which TG2 was knocked down was noted, this did not reach statistical significance perhaps due to the small number of tumors analyzed and to the rapid degradation of the chemotherapeutic agent *in vivo*.

As our results are based on observations of the effects of shRNA-mediated TG2 downregulation in PDA cells, we cannot differentiate between the specific functions of the protein contributing to response to chemotherapy in the pancreatic TME. Our previous work demonstrated that TG2 is enzymatically active in the pancreatic TME and pointed to its cross-linking activity as an important regulator of tumor progression [7]. Based on those results, we inferred that the enzymatic activity may be implicated in the response to chemotherapy. However, in the absence of experiments using potent TG2 enzymatic inhibitors active *in vivo*, our conclusions regarding the involvement of the catalytic activity of TG2 in the response to gemcitabine remain limited, and additional studies should be undertaken.

Differing from previous reports [29], our study did not show that TG2 knockdown sensitizes PDA cells to chemotherapy *in vitro*. A link between TG2 and chemoresistance was well established in breast cancer cells and attributed to activation of the NF-κB and AKT survival signaling pathways [28–30]. Mann et al. demonstrated that TG2 forms a complex with the regulatory protein IκBα causing its cross-linking [8]. In pancreatic cancer cells, the cross-linked IκBα dissociates from the Rel homology domain of NF-κB and is processed for proteasomal degradation, resulting in nuclear localization and constitutive activation of NF-κB. Additionally, TG2 was shown to directly interact with the phosphatase PTEN, causing inhibition of its phosphorylation at Ser^{380}, ubiquitination, and proteasomal degradation [29]. Collectively, TG2-induced activation of phosphatidylinositol 3-kinase/AKT and NF-κB survival signaling pathways is linked to resistance to chemotherapy and to the worse clinical outcomes observed in patients whose tumors harbor high levels of TG2. The analysis of the publically available pancreatic TCGA database presented here, demonstrating an inverse correlation between TG2 expression levels and survival of patients with PDA, is concordant with previous studies involving patient cohorts from single institutions [28] and supports the clinical relevance of our findings.

In all, our results demonstrate that TG2 secreted in the TME coordinates the cross talk between PDA cells and the stroma, promoting tumor growth and altering response to gemcitabine. This study supports TG2 inhibition in the pancreatic stroma to increase the antitumor effects of gemcitabine in difficult-to-treat pancreatic cancer.

Supplementary data to this article can be found online at http://dx.doi.org/10.1016/j.neo.2016.09.003.

Acknowledgements

We thank Drs. Dan Spandau, Jingwu Xie, and Murray Korc for reagents and Dr. Robert Emerson and Mrs. Bhadrani Chelladurai for technical assistance.

References

[1] Siegel R, Naishadham D, and Jemal A (2013). Cancer statistics, 2013. *CA Cancer J Clin* **63**, 11–30.
[2] Mehta K (2009). Biological and therapeutic significance of tissue transglutaminase in pancreatic cancer. *Amino Acids* **36**, 709–716.
[3] Verma A, Wang H, Manavathi B, Fok JY, Mann AP, Kumar R, and Mehta K (2006). Increased expression of tissue transglutaminase in pancreatic ductal adenocarcinoma and its implications in drug resistance and metastasis. *Cancer Res* **66**, 10525–10533.
[4] Feig C, Gopinathan A, Neesse A, Chan DS, Cook N, and Tuveson DA (2012). The pancreas cancer microenvironment. *Clin Cancer Res* **18**, 4266–4276.
[5] Korc M (2007). Pancreatic cancer-associated stroma production. *Am J Surg* **194**, S84–S86.
[6] Erkan M, Reiser-Erkan C, Michalski CW, and Kleeff J (2010). Tumor microenvironment and progression of pancreatic cancer. *Exp Oncol* **32**, 128–131.
[7] Lee J, Condello S, Yakubov B, Emerson R, Caperell-Grant A, Hitomi K, Xie J, and Matei D (2015). Tissue transglutaminase mediated tumor-stroma interaction promotes pancreatic cancer progression. *Clin Cancer Res* **21**, 4482–4493.
[8] Mann AP, Verma A, Sethi G, Manavathi B, Wang H, Fok JY, Kunnumakkara AB, Kumar R, Aggarwal BB, and Mehta K (2006). Overexpression of tissue transglutaminase leads to constitutive activation of nuclear factor-kappaB in cancer cells: delineation of a novel pathway. *Cancer Res* **66**, 8788–8795.
[9] Lu Z, Kleeff J, Shrikhande S, Zimmermann A, Korc M, Friess H, and Büchler MW (2000). Expression of the multidrug-resistance 1 (MDR1) gene and prognosis in human pancreatic cancer. *Pancreas* **21**, 240–247.

[10] O'Driscoll L, Walsh N, Larkin A, Ballot J, Ooi WS, Gullo G, O'Connor R, Clynes M, Crown J, and Kennedy S (2007). MDR1/P-glycoprotein and MRP-1 drug efflux pumps in pancreatic carcinoma. *Anticancer Res* **27**, 2115–2120.

[11] Banerjee S, Wang Z, Kong D, and Sarkar FH (2009). 3,3′-Diindolylmethane enhances chemosensitivity of multiple chemotherapeutic agents in pancreatic cancer. *Cancer Res* **69**, 5592–5600.

[12] Khanbolooki S, Nawrocki ST, Arumugam T, Andtbacka R, Pino MS, Kurzrock R, Logsdon CD, Abbruzzese JL, and McConkey DJ (2006). Nuclear factor-kappaB maintains TRAIL resistance in human pancreatic cancer cells. *Mol Cancer Ther* **5**, 2251–2260.

[13] Löhr M, Schmidt C, Ringel J, Kluth M, Müller P, Nizze H, and Jesnowski R (2001). Transforming growth factor-beta1 induces desmoplasia in an experimental model of human pancreatic carcinoma. *Cancer Res* **61**, 550–555.

[14] Mahadevan D and Von Hoff DD (2007). Tumor-stroma interactions in pancreatic ductal adenocarcinoma. *Mol Cancer Ther* **6**, 1186–1197.

[15] Olive KP, Jacobetz MA, Davidson CJ, Gopinathan A, McIntyre D, Honess D, Madhu B, Goldgraben MA, Caldwell ME, and Allard D, et al (2009). Inhibition of Hedgehog signaling enhances delivery of chemotherapy in a mouse model of pancreatic cancer. *Science* **324**, 1457–1461.

[16] Zemskov EA, Janiak A, Hang J, Waghray A, and Belkin AM (2006). The role of tissue transglutaminase in cell-matrix interactions. *Front Biosci* **11**, 1057–1076.

[17] Di Venere A, Rossi A, De Matteis F, Rosato N, Agrò AF, and Mei G (2000). Opposite effects of Ca(2+) and GTP binding on tissue transglutaminase tertiary structure. *J Biol Chem* **275**, 3915–3921.

[18] Pinkas DM, Strop P, Brunger AT, and Khosla C (2007). Transglutaminase 2 undergoes a large conformational change upon activation. *PLoS Biol* **5**, 2788–2796 [e-327].

[19] Iismaa SE, Mearns BM, Lorand L, and Graham RM (2009). Transglutaminases and disease: lessons from genetically engineered mouse models and inherited disorders. *Physiol Rev* **89**, 991–1023.

[20] Fesus L and Piacentini M (2002). Transglutaminase 2: an enigmatic enzyme with diverse functions. *Trends Biochem Sci* **27**, 534–539.

[21] Griffin M, Casadio R, and Bergamini CM (2002). Transglutaminases: nature's biological glues. *Biochem J* **368**, 377–396.

[22] Shipley LA, Brown TJ, Cornpropst JD, Hamilton M, Daniels WD, and Culp HW (1992). Metabolism and disposition of gemcitabine, and oncolytic deoxycytidine analog, in mice, rats, and dogs. *Drug Metab Dispos* **20**, 849–855.

[23] Kristjansen PE, Brown TJ, Shipley LA, and Jain RK (1996). Intratumor pharmacokinetics, flow resistance, and metabolism during gemcitabine infusion in ex vivo perfused human small cell lung cancer. *Clin Cancer Res* **2**, 359–367.

[24] Erkan M, Reiser-Erkan C, Michalski CW, Deucker S, Sauliunaite D, Streit S, Esposito I, Friess H, and Kleeff J (2009). Cancer-stellate cell interactions perpetuate the hypoxia-fibrosis cycle in pancreatic ductal adenocarcinoma. *Neoplasia* **11**, 497–508.

[25] Omary MB, Lugea A, Lowe AW, and Pandol SJ (2007). The pancreatic stellate cell: a star on the rise in pancreatic diseases. *J Clin Invest* **117**, 50–59.

[26] Huanwen W, Zhiyong L, Xiaohua S, Xinyu R, Kai W, and Tonghua L (2009). Intrinsic chemoresistance to gemcitabine is associated with constitutive and laminin-induced phosphorylation of FAK in pancreatic cancer cell lines. *Mol Cancer* **8**, 125.

[27] Miyamoto H, Murakami T, Tsuchida K, Sugino H, Miyake H, and Tashiro S (2004). Tumor-stroma interaction of human pancreatic cancer: acquired resistance to anticancer drugs and proliferation regulation is dependent on extracellular matrix proteins. *Pancreas* **28**, 38–44.

[28] Verma A, Guha S, Diagaradjane P, Kunnumakkara AB, Sanguino AM, Lopez-Berestein G, Sood AK, Aggarwal BB, Krishnan S, and Gelovani JG, et al (2008). Therapeutic significance of elevated tissue transglutaminase expression in pancreatic cancer. *Clin Cancer Res* **14**, 2476–2483.

[29] Verma A, Guha S, Wang H, Fok JY, Koul D, Abbruzzese J, and Mehta K (2008). Tissue transglutaminase regulates focal adhesion kinase/AKT activation by modulating PTEN expression in pancreatic cancer cells. *Clin Cancer Res* **14**, 1997–2005.

[30] Verma A and Mehta K (2007). Tissue transglutaminase-mediated chemoresistance in cancer cells. *Drug Resist Updat* **10**, 144–151.